Multichannel quantum-defect theory of double-minimum $^1\Sigma_g^+$ states in H_2. II. Vibronic-energy levels

S. C. Ross
Department of Physics, University of New Brunswick, P.O. Box 4400, Fredericton, New Brunswick, Canada E3B 5A3

Ch. Jungen
Laboratoire Aimé Cotton du CNRS, Université de Paris–Sud, 91405 Orsay, France
(Received 11 November 1993)

In the preceding paper [Phys. Rev. A **49**, 4353 (1994)] we obtained the quantum-defect matrix of the strongly interacting double-minimum states of H_2 by fitting to the *ab initio* clamped-nuclei electronic energies of Wolniewicz and Dressler [J. Chem. Phys. **82**, 3292 (1985), and private communication]. Yu, Dressler, and Wolniewicz have calculated the vibronic energies of the corresponding states using an approach involving the state-by-state evaluation of vibronic coupling, and the solution of a set of coupled equations. Here we calculate the vibronic energies using our quantum-defect matrix in a version of scattering theory known as multichannel quantum-defect theory (MQDT). This less traditional treatment involves both singly and doubly excited channels and reproduces the vibronic energies to almost the same precision as the coupled-equations approach. In addition, several refinements have been made to MQDT.

PACS number(s): 33.10.Cs, 33.10.Lb, 34.10.+x, 34.80.Kw

I. INTRODUCTION

In the previous paper in this series [1] (which we refer to as "RJ-I") we showed that the highly accurate *ab initio* clamped-nuclei potential-energy curves of Wolniewicz and Dressler [2,3] can be represented by a set of smooth quantum-defect functions. In this paper, we further show that these quantum-defect functions contain all of the information needed to calculate the energies of the vibrational levels in the corresponding electronic states.

The study of the $^1\Sigma_g^+$ electronic states of H_2 using more traditional molecular-dynamics techniques has been pursued in greatest detail by Dressler and co-workers (Ref. [4] and references therein, and, more recently, Refs. [5] and [6]). Their investigations involve, as a first step, performing highly accurate clamped-nuclei *ab initio* calculations of those electronic states chosen for inclusion in the calculations. Adiabatic corrections are then determined for each state and a set of nonadiabatic coupling functions is determined for each pair of states. In the $^1\Sigma_g^+$ states considered here the adiabatic corrections are as large as 860 cm^{-1} [2], and the vibrational levels are shifted by nonadiabatic effects by up to 190 cm^{-1} [4]. These strong interactions, and the resulting mixing in character of the states involved, means that it is inappropriate to refer to these states as being vibrational levels of particular electronic states. Instead we must refer to them as "vibronic" states. The final step in the traditional treatment is to include these interactions in a single global coupled-equations calculation.

These *ab initio* calculations have been very successful in reproducing the known energy levels of the *EF*, *GK*, and *H* states of H_2 and thus serve as a benchmark against which any other study of these levels must be compared. An important feature of these calculations is that they proceed on a state-by-state basis, explicitly accounting for the interactions between each pair of states. For Rydberg series, however, such an approach cannot be extended indefinitely because the number of mutually interacting states is infinite, with the density of states growing explosively as the total energy approaches the ionization limit.

In multichannel quantum-defect theory (MQDT), however, the notion of distinct states is replaced by the concept of a channel which incorporates an entire series of electronic Rydberg states in one entity. The quantum-mechanical functions describing the channels and their evolution with internuclear spacing is specified by quantum-defect functions. The quantum-defect functions thus provide a single uniform description of all the states in the channel, thereby allowing the theory to account for effects arising from the entire Rydberg series and the continuum lying above. The fact that the quantum defects describe the dependence of the electronic channel functions on the vibrational coordinate leads to their accounting for the strong adiabatic effects, and for the nonadiabatic interactions that occur between the vibrational levels of *different* electronic states, with no further information required. The vibronic energies that we obtain for the 2, 3, and 4 $^1\Sigma_g^+$ electronic states using the MQDT technique are of almost the same quality as those Dressler and co-workers obtained using the full molecular-dynamics apparatus. The MQDT results have an rms error of 6.0 cm^{-1} which compares very well to the value of 3.0 cm^{-1} obtained from the traditional approach [3,6].

II. THEORY

In 1977 Jungen and Atabek [7] (hereinafter referred to as "JA") presented the MQDT theory for rovibronic states of diatomic molecules, including provision for a direct treatment of electronic interaction. Ten years were

to pass until in 1987 we performed a calculation accounting for this interaction [8]. As described in RJ-I our 1987 calculation served as a "test of principle." In the following we show in detail how to use the quantum-defect matrix determined in RJ-I to calculate the energies of the first 39 vibronic levels of the excited $^1\Sigma_g^+$ states H_2, adapting the treatment to account for the energy dependence of the quantum-defect matrix. Many parts of the following development have previously been given, but are scattered throughout the literature. Our aim here is to draw the various pieces together and present a consistent overall picture of the method.

In MQDT the energy of the Rydberg electron is initially a free parameter so that rather than introducing basis functions corresponding to particular eigenstates of a molecule at specific bound-state energies, MQDT instead introduces basis functions in which all properties of the system are specified *except* the energy of the Rydberg electron. The resulting energy-dependent basis functions each correspond to what we call a "channel." These channel functions describe the asymptotic behavior of the molecule when the Rydberg electron is far from the ion core; they form a natural path to ionization and are called the "long-range" or "asymptotic" channels. It is only at the end of the theoretical development that boundary conditions are imposed on the channel functions and the energy eigenstates are obtained.

For a given total angular momentum, J, and Z-axis projection, M, the asymptotic channels are labeled by the electronic state of the combined ion+electron system i, and the vibrational-rotational state $v_i^+ N_i^+$ of the ion core. Thus each molecular channel function contains a factor $|iv_i^+ N_i^+\rangle^{JM}$ describing the degrees of freedom of the molecule other than the radial coordinator r, of the Rydberg electron. The vibrational motion in the ion core is assumed to be adiabatic, with nonadiabatic effects arising from interaction with the colliding Rydberg electron. It is also assumed that once the Rydberg electron is further than some finite distance from the core its motion occurs on a simple Coulomb potential-energy surface centered on the ion core and can, therefore, be described by a linear combination of a base pair of Coulomb functions. As in RJ-I we use the Coulomb base pair $f(r)$ and $h(r)$ (Ref. [9]) with which unphysical states having $n < l+1$, such as $1p$, $1d$, $2d$, etc., can usually be avoided in the MQDT. The Coulomb functions depend on the energy ϵ of the Rydberg electron, as well as on its l value. For a given total energy E of the molecule, the energy ϵ of the Rydberg electron is the difference between E and the energy of the ion core, i.e., when the molecule is in the channel $|iv_i^+ N_i^+\rangle$ we may write

$$\epsilon_{iv_i^+ N_i^+} = E - E^+_{iv_i^+ N_i^+} \ . \tag{1}$$

Because the l value of the electron is part of the electronic state i of the molecule we write it as l_i, and thus the Coulomb functions we use are $f_{l_i}(r,\epsilon_{iv_i^+ N_i^+})$ and $h_{l_i}(r,\epsilon_{iv_i^+ N_i^+})$.

The MQDT channel functions are now written as

$$\Psi^{JM}_{iv_i^+ N_i^+}(E) = f_{l_i}(r,\epsilon_{iv_i^+ N_i^+})|iv_i^+ N_i^+\rangle^{JM} + \sum_{jv_j^+ N_j^+} K_{iv_i^+ N_i^+, jv_j^+ N_j^+} \times h_{l_j}(r,\epsilon_{jv_j^+ N_j^+})|jv_j^+ N_j^+\rangle^{JM} \ . \tag{2}$$

They describe a molecule initially in the channel $|iv_i^+ N_i^+\rangle^{JM}$ which, upon the collision of the Rydberg electron with the core, enters a state involving a mixture of all channels $|jv_j^+ N_j^+\rangle^{JM}$. (Note that J and M remain good quantum numbers and are preserved in the collision so that the problem for each JM state is independent.) The collision induced admixture of channels in the MQDT basis functions is given by the real and symmetric full rovibronic reaction matrix K. In atomic MQDT the K matrix is often determined by fitting to experimental energy levels. For molecular problems the additional degree of freedom introduced by the vibrational motion means that such a fitting is not feasible due to the number of independent elements in the matrix. In the calculations described in the present work, we use a 200×200 K matrix to calculate the first 39 vibronic levels of the excited electronic states of the $^1\Sigma_g^+$ manifold. It is evident that 39 experimental energies are not sufficient to determine the 20 000 independent elements of the full K matrix.

JA, following earlier work in Refs. [10–12], showed that the solution to this problem lies in an examination of the physics of the actual collision. As the Rydberg electron falls towards the ion core it accelerates under the influence of the attractive Coulomb potential-energy function of the positive H_2^+ ion core. The resulting electron-ion collision is consequently very rapid with the result that during the collision the Rydberg electron interacts with a core that appears "frozen" at some particular configuration of the nuclei. The region wherein this is true we call the Born-Oppenheimer region because once the Rydberg electron is this close to the core the motion of *all* the electrons (rather than just the ion-core electrons) is separable from the vibrational-rotational motion. This means that the vibrational quantum number v_i^+ appropriate for the description of the asymptotic channels is replaced in the Born-Oppenheimer region by the internuclear spacing R seen by the Rydberg electron at the moment of collision. Similarly the total orbital angular momentum Λ around the molecular axis becomes a good quantum number, replacing the rotational angular momentum of the ion core, N_i^+, appropriate in the asymptotic region. The appropriate functions for describing the molecule in the Born-Oppenheimer region may, therefore, be written as $|iR\Lambda\rangle^{JM}$, instead of $|iv_i^+ N_i^+\rangle^{JM}$, in Eq. (2). These are referred to as "short-range" or "Born-Oppenheimer" functions. The fact that it is not necessary to introduce a strong energy (i.e., state) dependence in the quantum-defect matrix validates this picture and also validates the derivation in RJ-I of the quantum-defect matrix from clamped-nuclei (or Born-Oppenheimer) *ab initio* calculations.

By equating, in the Born-Oppenheimer region, the total wave function for the molecule expanded in asymptot-

ic channel functions with its expansion in Born-Oppenheimer channel functions, JA were able to determine the full K matrix of Eq. (2) in terms of the R-dependent electronic $K^{\Lambda}(R)$ matrix. This procedure amounts to carrying out a transformation from the laboratory to the molecular frame. A detailed discussion of the concept of the vibrational frame transformation and its relation to the energy dependence of the quantum defects has been presented by Greene [13]. The electronic quantum-defect matrix $\eta^{\Lambda}(R)$, determined in RJ-I for $\Lambda=0$, is connected to $K^{\Lambda}(R)$ via the relation between their elements

$$K_{ij}^{\Lambda}(R)=\tan\pi\eta_{ij}^{\Lambda}(R) . \tag{3}$$

The relationship between the electronic K^{Λ} matrices of Eq. (3) and the full K rovibronic matrix of Eq. (2) is implicit in Eq. (29) of JA, and is also given in Eq. (71) of Greene and Jungen [14]. Here we write it as

$$K_{iv_i^+N_i^+,jv_j^+N_j^+}=\int dR\ {}^{JM}\langle iv_i^+N_i^+|\left\{\sum_{\Lambda}|iR\Lambda\rangle^{JM}K_{ij}^{\Lambda}(R)\,{}^{JM}\langle jR\Lambda|\right\}|jv_j^+N_j^+\rangle^{JM} . \tag{4}$$

(The superscript Λ on the electronic K matrix distinguishes it from the full rovibronic matrix.)

Equation (4) directly reflects the physical picture underlying the frame transformation. The left-hand factor of the integrand corresponds to the system initially being in the asymptotic channel $|iv_i^+N_i^+\rangle^{JM}$. When the electron is close enough to the core the collision state satisfies the Born-Oppenheimer approximation and we enter the part of Eq. (4) in parenthesis. In this region the collision channels $|iR\Lambda\rangle^{JM}$ are appropriate for the description of the molecule. The incoming state is projected over the set of different collision channels states, as indicated by the summation over Λ and the integration over R. Once in this collision state the energy of the colliding Rydberg electron can lead to electronic rearrangement in the core via the off-diagonal elements of the electronic reaction matrix $K_{ij}^{\Lambda}(R)$, which connect different electronic states, i and j. Because the details of this rearrangement depend on the situation in the core at the moment of the collision the K_{ij} elements are functions of R as well as of Λ. When the Rydberg electron leaves the collision region the system is projected on to the asymptotic channel $|jv_j^+N_j^+\rangle^{JM}$, on the right of the integrand in Eq. (4). The full rovibronic reaction matrix of Eq. (4) thus leads to and accounts for a host of interactions between different rotational, vibrational, and electronic channels. At energies below threshold these interactions become apparent as perturbations of the rovibronic levels. A source of the power of MQDT resides in the fact that the limits corresponding to a coupled and uncoupled Rydberg electron are both directly and explicitly incorporated in the theory. The transformation between these two limits is embedded in the bra-kets ${}^{JM}\langle iv_i^+N_i^+|iR\Lambda\rangle^{JM}$ of Eq. (4) which will be specified below.

Once Eq. (4) has been used to perform the transformation from the electronic reaction matrix to the full rovibronic reaction matrix, the total MQDT wave function may then be written as a linear combination of the MQDT basis functions of Eq. (2)

$$\Psi^{JM}(E)=\sum_{iv_i^+N_i^+}Z_{iv_i^+N_i^+}\Psi^{JM}_{iv_i^+N_i^+}(E) . \tag{5}$$

An important aspect of this expansion for the total wave function is that it only involves channel functions evaluated "on the energy shell," i.e., at the energy E. This is possible because the channel functions of Eq. (2) are defined at all energies and already account for interchannel mixing *via* the incorporation of h Coulomb functions in their definitions through the rovibronic K matrix. Imposition of bound-state boundary conditions on the total wave function $\Psi^{JM}(E)$ of Eq. (5) results in the following well-known [9] determinantal condition for the bound-state energies

$$\left|K+\frac{\tan(\pi\nu)}{A(\nu)}\right|=0 , \tag{6}$$

where ν is the effective quantum number

$$\nu_{iv_i^+N_i^+}=\left[-\frac{1}{2\epsilon_{iv_i^+N_i^+}}\right]^{1/2} \tag{7}$$

(see Sec. III C 2 for the slight modification of this relation actually used in our calculations), and $A(\nu)$ arises from our use of the h Coulomb function [9]

$$A(\nu_{iv_i^+N_i^+})=\prod_{j=0}^{l_i}\left[1-\frac{j^2}{\nu^2_{iv_i^+N_i^+}}\right] . \tag{8}$$

$\tan(\pi\nu)$ and $A(\nu)$ are the diagonal matrices

$$\begin{aligned}[\tan(\pi\nu)]_{iv_i^+N_i^+,jv_j^+N_j^+}&=\delta_{ij}\delta_{v_i^+v_j^+}\delta_{N_i^+N_j^+}\tan(\pi\nu_{iv_i^+N_i^+}) ,\\ [A(\nu)]_{iv_i^+N_i^+,jv_j^+N_j^+}&=\delta_{ij}\delta_{v_i^+v_j^+}\delta_{N_i^+N_j^+}A_{l_i}(\nu_{iv_i^+N_i^+}) .\end{aligned} \tag{9}$$

Equation (6) is just the rovibronic generalization of the equivalent electronic Eq. (9) of RJ-I and it specifies the rovibronic bound-state energies of the molecule. The procedure is to first use Eq. (3) to calculate the electronic K matrix from the electronic η quantum defect we obtained in RJ-I. (For states involving values of J other than 0 the appropriate η matrices for Λ other than 0 have to be determined. This poses no problem.) The electronic K matrix is then substituted into Eq. (4) and the full rovibronic K matrix is calculated as described in Sec. III. With the full rovibronic K matrix the determinant in Eq.

(6) may be calculated for any given total energy E by use of Eqs. (7) to (9), with the energy ϵ of the Rydberg electron as seen in each channel given by Eq. (1). If the determinant is zero then the trial energy E corresponds to the energy of a rovibronic bound state of the molecule. If it differs from zero then the energy does not correspond to a rovibronic bound state and another energy may be tried. This search procedure is automated in the computer program.

The energy search procedure was guided by experimental results, using a grid spacing of several wavenumber units in the region of each experimental energy. Because it is possible to miss levels care must be taken. Two independent formulations of the problem were used, one in terms of the *tangent* function, the other in terms of *sine* and *cosine* functions as in JA. These have different behaviors around the eigenenergies and facilitate the search for problematic levels. Occasionally "false" levels corresponding to high lying vibrational states of the unphysical $2d$ state appear. This is presumably due in part to the finite basis set used in the calculations. The false levels, however, are easily identified by examination of the eigenvectors, and are then discarded.

III. CALCULATION OF THE ROVIBRONIC-ENERGY LEVELS

In this section we describe the details of the procedure used to calculate the full rovibronic K matrix of Eq. (4) and subsequently the rovibronic bound-state energies using Eq. (6)

A. Frame transformation

We begin by specifying the channel factors that appear in Eq. (2). These are given by

$$|iv_i^+ N_i^+\rangle^{JM} = |n_i^+ \Gamma_i^+ \Lambda_i^+\rangle |v_i^+; iN_i^+\rangle \sum_m (N_i^+ M - m, l_i m | JM) |N_i^+ \Lambda_i^+ M - m\rangle |l_i m\rangle' \ . \tag{10}$$

Here $|n_i^+ \Gamma_i^+ \Lambda_i^+\rangle$ is the electronic core state, with n_i^+ numbering core states of angular-momentum projection Λ_i^+ and of symmetry Γ_i^+. Thus, n_i^+, Γ_i^+, and Λ_i^+, along with l_i, are contained in the compound index i. In the present example, the core states involved are the $1\sigma_g$ and $1\sigma_u$ states of H_2^+. $|v_i^+; iN_i^+\rangle$ are the adiabatic vibrational core wave functions which depend on both the electronic state implicit in the index i and on the core rotational quantum number N_i^+. Finally, the angular momenta of the ion core and of the Rydberg electron are coupled by standard Clebsch-Gordon coefficients to yield a given J and M. The ion-core rotational functions $|N_i^+ \Lambda_i^+ M_i^+\rangle$ correspond to the isomorphic linear molecule Hamiltonian [15], whereas the Rydberg electron is described by standard spherical harmonics $|l_i m\rangle'$. The prime denotes quantization with respect to the space-fixed Z axis.

The short-range functions that appear in Eq. (4) for the rovibronic K matrix are given by

$$|iR\Lambda\rangle^{JM} = |n_i^+ \Gamma_i^+ \Lambda_i^+\rangle |R\rangle |l_i \Lambda - \Lambda_i^+\rangle |J\Lambda M\rangle \ . \tag{11}$$

Here R is the internuclear distance as before and $|J\Lambda M\rangle$ is a rotational wave function which now describes the rotational of the whole molecule, including the Rydberg electron. Correspondingly the spherical harmonic $|l_i \Lambda - \Lambda_i^+\rangle$ refers to quantization in the molecular frame, and Λ is the total angular-momentum component along the molecular axis. The core electronic wave functions in Eq. (11) are the same as in the asymptotic expression Eq. (10).

The two expressions, Eqs. (10) and (11), must now each be combined to yield states of definite total parity. Letting $\not{\epsilon}$ represent the parity ($\pm$) of the total wave function and $\not{\epsilon}^+$ the electronic parity of the core (-1 for Σ^- states, $+1$ otherwise), the symmetric combinations for the asymptotic region are found to be *symmetrized asymptotic basis functions,*

$$|iv_i^+ N_i^+; \not{\epsilon}\rangle^{JM} = \frac{1}{\sqrt{2(1+\delta_{\Lambda^+ 0})}} \sum_m (N_i^+ M - m, l_i m | JM) \times \{ |n_i^+ \Gamma_i^+ \Lambda_i^+\rangle |N_i^+ \Lambda_i^+ M - m\rangle + \not{\epsilon}\not{\epsilon}^+ (-1)^{N_i^+ + l_i} |n_i^+ \Gamma_i^+ \overline{\Lambda_i^+}\rangle |N_i^+ \overline{\Lambda_i^+} M - m\rangle \} |l_i m\rangle' |v_i^+; iN_i^+\rangle \ , \tag{12}$$

where all quantum numbers other than m and M are nonnegative, and $\overline{\Lambda_i^+} = -\Lambda_i^+$.

For the Born-Oppenheimer region there are two distinct types of symmetrized basis functions as follows: *symmetrized Born-Oppenheimer basis functions,*

$$|iR\Lambda; \oplus \not{\epsilon}\rangle^{JM} = \frac{1}{\sqrt{2(1+\delta_{\Lambda^+ 0}\delta_{\Lambda 0})}} \{ |n_i^+ \Gamma_i^+ \Lambda_i^+\rangle |l_i \Lambda - \Lambda_i^+\rangle |J\Lambda M\rangle + \not{\epsilon}\not{\epsilon}^+ (-1)^J |n_i^+ \Gamma_i^+ \overline{\Lambda_i^+}\rangle |l_i \overline{\Lambda - \Lambda_i^+}\rangle |J\overline{\Lambda} M\rangle \} |R\rangle \ , \tag{13}$$

$$|iR\Lambda;\ominus\not{\epsilon}\rangle^{JM}=\frac{1}{\sqrt{2(1+\delta_{\Lambda^+0}\delta_{\Lambda 0})}}\{|n_i^+\Gamma_i^+\overline{\Lambda_i^+}\rangle|l_i\Lambda+\Lambda_i^+\rangle|J\Lambda M\rangle+\not{\epsilon}\not{\epsilon}^+(-1)^J|n_i^+\Gamma_i^+\Lambda_i^+\rangle|l_i\overline{\Lambda+\Lambda_i^+}\rangle|J\overline{\Lambda}M\rangle\}|R\rangle\ .$$

Here, the $\oplus$ functions correspond to parallel angular-momentum projections of the ion core and the Rydberg electron, while the $\ominus$ functions correspond to antiparallel projections. The $\ominus$ functions only occur for non-Σ cores combined with non-σ electrons and, thus, do not play a role in the current work.

Using these expressions the evaluation of the rotational frame transformation required for the full K matrix of Eq. (4), is performed following the procedure of Chang and Fano [16]. The resulting elements of the frame transformation are

$$\begin{aligned}
&{}^{JM}\langle iv_i^+N_i^+;\not{\epsilon}|iR\Lambda;\oplus\not{\epsilon}\rangle^{JM}\\
&\quad=\frac{1}{\sqrt{(1+\delta_{\Lambda_i^+0})(1+\delta_{\Lambda_i^+0}\delta_{\Lambda 0})}}\left[\frac{2N_i^++1}{2J+1}\right]^{1/2}[1+\delta_{\Lambda_i^+0}\not{\epsilon}\not{\epsilon}^+(-1)^{N_i^++l_i}](N_i^+\Lambda_i^+,l_i\Lambda-\Lambda_i^+|J\Lambda)\langle v_i^+;iN_i^+|R\rangle\ ,\\
&{}^{JM}\langle iv_i^+N_i^+;\not{\epsilon}|iR\Lambda;\ominus\not{\epsilon}\rangle^{JM}\\
&\quad=\frac{1}{\sqrt{(1+\delta_{\Lambda_i^+0})(1+\delta_{\Lambda_i^+0}\delta_{\Lambda 0})}}\left[\frac{2N_i^++1}{2J+1}\right]^{1/2}[\delta_{\Lambda_i^+0}+\not{\epsilon}\not{\epsilon}^+(-1)^{N_i^++l_i}](N_i^+\overline{\Lambda_i^+},l_i\Lambda-\overline{\Lambda_i^+}|J\Lambda)\langle v_i^+;iN_i^+|R\rangle\ .
\end{aligned}\tag{14}$$

This frame transformation is diagonal in i, J, M, and $\not{\epsilon}$, and corresponds to that given by Child and Jungen [17]. Note that these authors corrected an error in the original derivation by Chang and Fano.

B. Evaluation of full rovibronic reaction matrix

In order to evaluate the full rovibronic K matrix of Eq. (4) one must substitute the frame transformation of Eqs. (14) into (4). Factoring out the terms that do not depend on the internuclear distance R and using Eq. (3) we find that the integral to be performed is

$$\begin{aligned}
&\int\langle v_i^+;iN_i^+|R\rangle K_{ij}^{\Lambda}(R)\langle R|v_j^+;jN_j^+\rangle dR\\
&\quad=\langle v_i^+;iN_i^+|\tan\pi\eta_{ij}^{\Lambda}(R)|v_j^+;jN_j^+\rangle\ .
\end{aligned}\tag{15}$$

A difficulty arises in the evaluation of these elements because of the appearance of the tangent function. Since the η defects can, and in the present case do, cross half integer values the integrand is singular. In the case of a single electronic channel, Du and Greene [18] use a technique of evaluation based on the spectral decomposition of the $\eta(R)$ operator which results in the evaluation of integrals involving $\eta(R)$, instead of $\tan\pi\eta(R)$. Because of the smoothness with R of the quantum defects [see, for example, Fig. 2 of JA or Fig. 3(a) of RJ-I] these integrals pose no numerical difficulty. In this work, we generalize Du and Greene's technique to additionally account for electronic channel mixing. Derived in Appendix A, this technique involves the following three steps.

(1) For each Λ, the electronic matrix $K_{ij}^{\Lambda}(R)=\tan\pi\eta_{ij}^{\Lambda}(R)$ is diagonalized on a relatively coarse grid of R values by the matrix $V^{\Lambda}(R)$. The arctangent of the resulting diagonal matrix is calculated (equivalent, for a diagonal matrix, to taking the arctangent of each diagonal element), thereby removing the poles that occur in the electronic reaction matrix $K^{\Lambda}(R)$, and the result is divided by π to yield the diagonal matrix of "eigenquantum defects" η^{Λ}. Care is taken in evaluating the arctangent to ensure continuity with R of the diagonal elements η_{α}^{Λ}. The inverse transformation is applied to the matrix of eigenquantum defects to yield the smooth electronic matrix

$$\begin{aligned}
M^{\Lambda}(R)&=V^{\Lambda}(R)[\eta^{\Lambda}(R)]V^{\Lambda^{\dagger}}(R)\\
&=V^{\Lambda}(R)\left[\frac{1}{\pi}\arctan(V^{\Lambda^{\dagger}}(R)K^{\Lambda}(R)V^{\Lambda}(R))\right]\\
&\quad\times V^{\Lambda^{\dagger}}(R)\ ,
\end{aligned}\tag{16}$$

which is splined onto a fine grid of R values in preparation for numerical integration in step 2.

(2) The smoothness with R of the $M^{\Lambda}(R)$ matrix allows the straightforward Simpson's rule evaluation of the matrix elements of $M^{\Lambda}(R)$ in terms of the adiabatic ionic vibrational functions $|v_i^+;iN_i^+\rangle$. The matrix elements are multiplied by the appropriate rotational parts of the frame transformation of Eq. (14) and summed over Λ to yield the complete rovibronic quantum-defect matrix M (where for clarity we neglect symmetry)

$$\begin{aligned}
M_{iv_i^+N_i^+,jv_j^+N_j^+}&=\sum_{\Lambda}{}^{JMi}\langle N_i^+|\Lambda\rangle^{JMi}\\
&\quad\times\langle v_i^+;iN_i^+|M_{ij}^{\Lambda}(R)|v_j^+;jN_j^+\rangle\\
&\quad\times{}^{JMj}\langle\Lambda|N_j^+\rangle^{JMj}\ .
\end{aligned}\tag{17}$$

(3) The full rovibronic K matrix of Eq. (4) is then recovered by diagonalizing M with the unitary matrix U, taking tangentπ of the diagonal result, and then applying the inverse transformation

$$K=U\tan(\pi U^{\dagger}MU)U^{\dagger}\ .\tag{18}$$

The appearance of the tangentπ in this step is a formal

reversal of the $1/\pi$arctangent of step 1, and is therefore what returns us to the K matrix.

Thus, the integration in Eq. (15) of the possibly ill-behaved $\tan\pi\eta(R)$ functions is replaced by Eq. (17) by integrals involving well behaved R dependent functions. The price paid for this simplification is the diagonalization in Eq. (18) of the large (200×200 here) rovibronic quantum-defect matrix of Eq. (17), a step not needed in a direct evaluation of the integrals involving the tangent function.

The quantum-defect matrix determined in RJ-I, and which we use here, involves a linear dependence on energy of the η_{ss} defect. A particular advantage of the evaluation technique just described is that if the energy dependence of the quantum defects is smooth then this smoothness carries through to the M matrix evaluated in step 2 [Eq. (17)]. The energy dependence can, therefore, be accounted for by performing a preparatory calculation of M on a coarse grid of Rydberg electron energies, ϵ. Because this matrix is a smooth function of energy, interpolation to determine its elements at other energies is straightforward and accurate. Thus, in the energy search calculation, each element of M is determined by interpolating between its precalculated values. Following Gao and Greene [19], we use the energy-modified vibrational frame transformation, i.e., we use the arithmetic mean, $\bar{\epsilon}=(\epsilon_i+\epsilon_j)/2$, of the channel energies in evaluating $M_{ij}^{\wedge}(R)$ when performing the integrals of Eq. (17). In this way steps 1 and 2, which include the numerical integrations, only need to be performed on the coarse energy grid. In the current work of a grid of three points over the energy range $\epsilon=-0.25$–0.00 a.u. combined with quadratic interpolation resulted in essentially identical results as obtained by a cubic spline interpolation over five points. Note, however, that in the case of an energy dependence the disadvantage of having to diagonalize the large M matrix in Eq. (18) is repeated for each energy.

Our results show that this method of accounting for the energy dependence of the quantum-defect matrix represents a significant improvement over that used in our proof of principle calculation [8], wherein the η_{ss} quantum defect was taken as a step function of energy, having a single step between the $2s$ and $3s$ diabatic states. The linear energy dependence of the quantum defect used here is also more appropriate than the step energy dependence used there. This better treatment, combined with the improvement in the fitted quantum-defect functions obtained in RJ-I, is the origin of the significant improvement in the vibronic results obtained below.

C. Remaining effects

In their paper on the use of MQDT to account for rovibronic interaction in H_2, JA begin their development of the theory by partitioning the molecular Hamiltonian in a manner different from that of the traditional quantum-mechanical treatment [see Eq. (3) of JA]. Their partitioning involved identifying the parts of the Hamiltonian relating to the H_2^+ ion core, the Rydberg electron, and to the interaction between the ion core and the Rydberg electron. MQDT, applied without correction, accounts for the most important of the terms in each of these parts of the Hamiltonian. The remaining terms can generally be accounted for by slight modifications of the MQDT procedure. Using the notation of JA, we may identify the terms neglecting in the "pure" MQDT for homonuclear H_2 as the following (in a.u.):

$$H_{\text{missing}}^{\text{Ion}}=\frac{1}{2\mu}\nabla_{R\Theta\Phi}^{+2}-\frac{1}{8\mu}\nabla_2^2\,,$$
$$H_{\text{missing}}^{\text{Rydberg}}=\frac{1}{8\mu}\nabla_1^2\,, \tag{19}$$
$$H_{\text{missing}}^{\text{Interaction}}=\frac{1}{4\mu}\nabla_1\cdot\nabla_2\,,$$

where the subscripts "1" and "2" represent the Rydberg electron and the core electron, respectively, and μ is the reduced mass of the H_2 molecule. Because these "missing" terms are all relatively small we consider them in a diagonal (or adiabatic) approximation by accounting for their expectation values. In Secs. III C 1–III C 3 we discuss each of these terms in turn, and how they are accounted for in the MQDT treatment. Finally, we discuss the consequences of the neglect of l mixing at large R and of relativistic effects in the H_2^+ ion in Secs. III C 4 and III C 5, respectively.

1. $H_{\text{missing}}^{\text{Ion}}$

As described in JA, the elements missing from the ionic part of the MQDT procedure, and given above as $H_{\text{missing}}^{\text{Ion}}$, can be accounted for by a standard adiabatic approximation in which the expectation value $\langle H_{\text{missing}}^{\text{Ion}}(R)\rangle$ is determined for each electronic state of the ion as a function of R, neglecting coupling with other states. These expectation values are the R-dependent adiabatic corrections which are added to the ionic potential curves for the determination of the adiabatically corrected vibrational wave functions and energies of the ion. It is these adiabatic vibrational wave functions which were used in JA and which we use to calculate the full rovibronic K matrix of Eq. (4), using the procedure of Sec. III B. The adiabatic vibrational energies are used in Eq. (1).

The present problem involves two electronic states of the H_2^+ ionic core, the $1\sigma_g$ and the $1\sigma_u$ states. Although the adiabatic corrections we use for the $1\sigma_g$ state are well known [20], those of the $1\sigma_u$ state of the H_2^+ ion core are apparently not available in tabular form in the literature and we calculated them ourselves as described in Appendix B.

This term is responsible for quite uniform increases in the energies of the calculated ionic levels, of the order of roughly 60 cm^{-1} around equilibrium for the $1\sigma_g$ state, and around 120 cm^{-1} at the same $R=2$ a.u. value for the $1\sigma_u$ state. These increases carry through to the calculated molecular levels.

2. $H_{\text{missing}}^{\text{Rydberg}}$

This term, the "normal mass effect," is clearly proportional to the kinetic-energy operator for the Rydberg

electron,

$$H_{\text{missing}}^{\text{Rydberg}}=\frac{1}{8\mu}\nabla_1^2=\frac{1}{4\mu}\left[\frac{1}{2(m_e=1)}\nabla_1^2\right]=\frac{1}{4\mu}T_1 \ . \quad (20)$$

We account for this term in essentially the same way as we did for $H_{\text{missing}}^{\text{Ion}}$, by including its expectation value in the MQDT treatment. In the present work, we do this in a more complete way than has previously been done. In JA, for example, the expectation value $\langle H_{\text{missing}}^{\text{Rydberg}}\rangle$ was determined using the virial theorem for the electron alone, as is done for atoms [21]. Here the fact that our MQDT determination of the quantum defects in RJ-I relied on the Born-Oppenheimer approximation, in which the nuclei are held "clamped," is also taken into account in the calculation of the electronic expectation value of $\langle H_{\text{missing}}^{\text{Rydberg}}\rangle$.

The virial theorem and its application to the clamped-nuclei approximation is well known from standard texts [22]. Using the virial theorem the expectation value of the kinetic-energy operator is given by

$$\langle T\rangle=-E(R)-R\frac{dE(R)}{dR} \ , \quad (21)$$

where $E(R)$ is the electronic energy of the state. We may also apply this result to the H_2^+ ion core, denoting the related core quantities with a superscript "+,"

$$\langle T^+\rangle=-E^+(R)-R\frac{dE^+(R)}{dR} \ . \quad (22)$$

Subtracting this equation from the previous one, remembering that Rydberg electron has total energy ϵ and is indicated by the index "1," we obtain,

$$\begin{aligned}\langle T_1\rangle&=\langle T\rangle-\langle T^+\rangle\\&=-[E(R)-E^+(R)]-R\frac{d}{dR}[E(R)-E^+(R)]\\&=-\left[\epsilon(R)+R\frac{d\epsilon(R)}{dR}\right] \ , \end{aligned} \quad (23)$$

and hence, in atomic units ($m_e=1$),

$$\langle H_{\text{missing}}^{\text{Rydberg}}\rangle=-\frac{1}{4\mu}\left[\epsilon(R)+R\frac{d\epsilon(R)}{dR}\right] \ . \quad (24)$$

This quantity represents the amount by which the calculated energies must be increased. Due to the different forms of the two terms appearing in Eq. (24) their incorporation into our MQDT treatment is handled in different ways and so discussed separately.

The first term, $-\epsilon(R)/4\mu$, corresponds to a proportional change in the energy of the Rydberg electron

$$\epsilon^{\text{Corrected}}(R)=\left[1-\frac{1}{4\mu}\right]\epsilon(R) \ . \quad (25)$$

It is accounted for in the usual manner by decreasing the Rydberg energy by a factor of $(1-1/4\mu)$ throughout the rovibronic treatment [7]. This amounts to shifting the Rydberg constant in Eq. (7) from the value $\frac{1}{2}$ a.u., appropriate for infinite mass, to the value $\frac{1}{2}(1-1/4\mu)$ a.u., a difference of just under 30 cm^{-1} for H_2.

The second term of Eq. (24) is not simply proportional to ϵ and can therefore not be absorbed into the Rydberg constant. Instead, we adjust the energies obtained in the MQDT by changing the quantum defects. In Appendix C we show that this small electronic correction can be treated in a diagonal approximation by correcting the diagonal quantum defects $\eta(R)$ according to

$$\eta^{\text{Corrected}}=\eta+\Delta\eta=\eta-\frac{1}{4\mu}R\frac{\partial\eta}{\partial R} \ . \quad (26)$$

In this work, the derivative correction of Eq. (26) is applied. Its effect on the calculated rovibronic energies was determined by comparing the results of including or not including it. Such a comparison shows that this correction improves the results for the lowest levels of the F state by up to 9 cm^{-1}. The overall rms error of the calculated levels is only slightly improved by the inclusion of this correction, but the average error decreases from 3.9 to 0.3 cm^{-1}.

3. $H_{\text{missing}}^{\text{Interaction}}$

This term is called the "specific mass effect" and is discussed in some detail in JA. The integrand in $H_{\text{missing}}^{\text{Interaction}}$ involves a coupling between the wave function of the core electron and that of the Rydberg electron. For Rydberg states, these wave functions only overlap slightly and, thus, this term is expected to be small. Wolniewicz and Dressler [2] refer to this term as H_3' and have calculated it for the EF, GK, and $H\bar{H}$ electronic states and even for these low Rydberg states it is quite small (absolute values <2.3 cm^{-1} for the EF state, <7.2 cm^{-1} for the GK state, and <1.9 cm^{-1} for the $H\bar{H}$ state). This term is, therefore, of approximately the same size as the precision of the fitting to the Born-Oppenheimer potentials in RJ-I. At higher energy the overlap between the core and Rydberg electron wave functions becomes even smaller and, therefore, this term will rapidly become even less important. We therefore neglect it.

4. *Neglect of l mixing at large R*

Another shortcoming of the present treatment is the restriction of the partial wave expansion to $l\leq 2$ which clearly becomes inadequate as R becomes large. JA have shown that because the quantum defects still reproduce the accurate Born-Oppenheimer potential-energy functions at large R, the consequences of this restriction are limited to the adiabatic corrections. However, the physical content of the quantum-defect functions as representing the partial-wave expansion is lost to some extent. Another feature at large R is that the physically appropriate description of the Rydberg electron is that it orbits one or the other of the dissociating atoms, rather than an H_2^+ ion core. Thus, in this region, the mass appearing in Eq. (25) should now be that of the H nucleus, rather than that of the united atom (He). In the limit of large R this corresponds to a missing correction $\frac{1}{4}(\mathcal{R}_\infty-\mathcal{R}_{H_2})$ to the energy, where $\mathcal{R}_\infty$ is the Rydberg constant for infinite mass and $\mathcal{R}_{H_2}$ that corrected for the

finite mass of H_2. JA showed that for $n=2$ this causes levels near dissociation, and thus sampling large R geometries, to be calculated 7.5 cm^{-1} too low. They indeed found this to be the case in the $2p\pi\, C\,{}^1\Pi_u$ state (cf. Fig. 6 of JA). This same behavior occurs here for high lying vibrational levels of the $F^1\Sigma_g^+$ state, as will be discussed in the Discussion of Results.

5. *Relativistic effects in H_2^+*

Relativistic effects in the H_2^+ ion core can be accounted for by simply using vibrational energies incorporating these effects when evaluating Eq. (1) for use in Eq. (7). Such energies, however, are only available for the physical vibrational levels, which form only a small subset of the 200 vibrational levels used in our calculation. Furthermore, these relativistic corrections are small [23] and their inclusion or noninclusion has only a small effect on the energies obtained in our calculations. The results quoted in Table I do not include the relativistic effects of the ion.

D. Computational details

The determination of the full rovibronic reaction matrix of Eq. (4), by the procedure of Sec. III B, requires vibrational wave functions for the $1\sigma_g$ and $1\sigma_u$ states of the H_2^+ ion. These we determine using Numerov-Cooley numerical integration [24] over the range $R=0.1-12.0$ a.u., on a grid of 999 points, incorporating the adiabatic corrections corresponding to $\langle H^{\rm Ion}_{\rm missing}\rangle$ in the ionic potential-energy curves. For the $1\sigma_g$ state, this procedure is straightforward and in our calculations we have included the levels $v=0-44$ for both the s and d channels built on this ionic state. The p channel, however, is built on the repulsive $1\sigma_u$ state which does not support bound vibrational levels in the region in which we require vibrational basis functions. We handle this situation as before [8], by fixing the logarithmic derivative of the vibrational functions to some constant value at the outer R value. This results in an orthonormal vibrational basis set that samples the vibrational continuum over a finite range of R and at discrete energies. We chose to include those vibrational functions that are zero at the R value forming the outer bound for our calculation and have included the levels $v=0-109$. These vibrational basis sets ensure a complete coverage of the R range important for the states considered in this work.

In RJ-I we determined the η^Λ matrix for $\Lambda=0$. In the present work, we restrict our attention to $J=0$ levels with the consequence that the summation over Λ in Eq. (4) collapses to this single value. In addition, we have restricted the treatment of $l\le 2$. Higher l states are nonpenetrating and, thus, are not normally strongly involved in configuration mixing for moderate values of R. Under these circumstances the symmetrized Born-Oppenheimer and asymptotic basis functions of Eqs. (12) and (13) are

Born-Oppenheimer	*Asymptotic*
$\lvert 1\sigma_g\rangle\lvert J=0\ \Lambda=0\ M\rangle\lvert l=0\ \sigma\rangle$:	$\lvert 1\sigma_g\rangle\sum_m (N^+=0\ M-m,\ l=0\ m)\lvert N^+=0\ 0\ M-m\rangle\lvert l=0\ m\rangle'$,
$\lvert 1\sigma_g\rangle\lvert J=0\ \Lambda=0\ M\rangle\lvert l=2\ \sigma\rangle$:	$\lvert 1\sigma_g\rangle\sum_m (N^+=2\ M-m,\ l=2\ m)\lvert N^+=2\ 0\ M-m\rangle\lvert l=2\ m\rangle'$,
$\lvert 1\sigma_u\rangle\lvert J=0\ \Lambda=0\ M\rangle\lvert l=1\ \sigma\rangle$:	$\lvert 1\sigma_u\rangle\sum_m (N^+=1\ M-m,\ l=1\ m)\lvert N^+=1\ 0\ M-m\rangle\lvert l=1\ m\rangle'$. (27)

Because the rotational frame transformation is diagonal in l it reduces for $J=0$ to the value unity and there is, therefore, a one-to-one correspondence between the Born-Oppenheimer and asymptotic basis functions as indicated in Eq. (27). Thus, the incoming asymptotic channels each project onto a single Born-Oppenheimer channel in the present case. In the core region, the nondiagonal quantum-defect matrix leads to configuration mixing between different Born-Oppenheimer states with $\Lambda=0$ *via* the full rovibronic reaction matrix of Eq. (4). For $J\neq 0$ the one-to-one correspondence between asymptotic and Born-Oppenheimer rotational channels is lost and further mixing due to the rotational part of the frame transformation becomes possible as will be discussed with regard to the $3d$ complex in the next paper in this series.

Physical constants used are from Ref. [25]. The quantum-defect calculations yield vibronic energies relative to the $v^+=0$, $N^+=0$, $1\sigma_g$ level of H_2^+. We convert these to energies above the $v=0$, $J=0$, level of neutral H_2 by adding the theoretical ionization potential of H_2 of Kołos, Szalewicz, and Monkhorst, viz., 124 417.512 cm^{-1} [26]. The $1\sigma_g$ and $1\sigma_u$ potential-energy curves of H_2^+ are from the work of Wind [27] and Bates, Ledsham, and Stewart [28], respectively.

IV. DISCUSSION OF RESULTS

The comparison with experiment of the $J=0$ vibronic energies that we have calculated is presented in Table I. For comparison this table also includes results obtained by Yu, Dressler, and Wolniewicz [3,6] using the coupled equations technique. Both calculations are seen to be in extremely good agreement with experiment. The comparison is illustrated by Fig. 1. In each part of this figure we show the observed minus calculated energies in wave

numbers of the first 39 vibrational levels of the excited electronic states of $^1\Sigma_g^+$ symmetry as functions of the total energy of the vibrational state relative to the $J=0$, $v=0$ level of the $\tilde{X}\,^1\Sigma_g^+$ ground state. This is done for different theoretical approaches and approximations. Only the first 39 states are considered because the 40th state is not observed experimentally, and higher states involve large values of R and were not appropriate to consider here.

Figure 1(a) compares the results obtained in the Born-Oppenheimer calculation and those obtained from the present vibronic MQDT calculations. Remember that both of these calculations are based on the same *ab initio* Born-Oppenheimer (or "clamped-nuclei") potential-energy curves. In the Born-Oppenheimer calculation the

TABLE I. Comparison of observed and calculated vibronic energies of H_2 (cm^{-1}).

Vibronic state	Vibronic energy[a]	(Observed) − (Calculated) MQDT	(Observed) − (Calculated) Coupled equations[a]
$E0$	99 164.782	4.4	−0.5
$F0$	99 363.92	1.3	−0.4
$F1$	100 558.92	0.1	−0.4
$E1$	101 494.749	5.0	−1.0
$F2$	101 698.93	0.3	−0.5
$F3$	102 778.28	−1.2	−0.4
$E2$	103 559.59	−2.3	−1.4
$F4$	103 838.54	0.0	−0.8
$F5$	104 730.61	−3.1	−0.9
$EF9$	105 384.90	−0.1	−2.1
$EF10$	105 966.16	3.0	−1.8
$EF11$	106 713.07	2.6	−1.7
$EF12$	107 425.87	4.8	−2.0
$EF13$	108 098.56	6.1	−2.1
$EF14$	108 793.55	5.7	−2.4
$EF15$	109 493.90	6.3	−2.3
$EF16$	110 163.38	7.3	−1.5
$EF17$	110 794.19	6.2	−1.1
$EF18$	111 370.69	−4.6	−4.7
$GK0$	111 628.81	−7.5	−3.6
$GK1$	111 812.665	1.1	−2.9
$EF19$	112 106.09	7.2	−1.6
$EF20$	112 711.80	5.2	−3.6
$H0$	112 957.57	−10.3	−1.0
$GK2$	113 258.24	2.7	−7.0
$EF21$	113 393.50	2.5	−2.0
$EF22$	113 861.40	4.7	−1.7
$GK3$	114 044.66	−1.3	−10.2
$EF23$	114 510.539	4.6	−5.5
$EF24$	115 024.834	1.3	−1.3
$GK4$	115 099.84	−16.0	−9.2
$H1$	115 251.52	5.1	−6.2
$EF25$	115 563.70	−1.4	−5.8
$EF26$	116 041.59	−1.4	−6.5
$GK5$	116 164.81	1.7	−7.8
$EF27$	116 508.24	−5.2	−4.5
$EF28$	116 915.36	−16.8	−9.8
$GK6$	117 081.43	11.4	−10.4
$H2$	117 297.02	6.7	−8.0

[a]Values from Ref. 3.

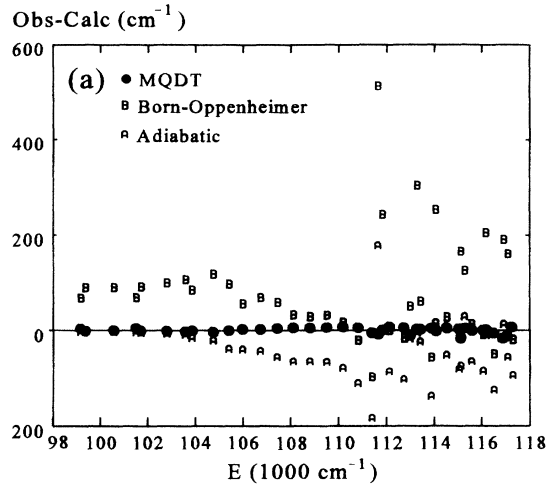

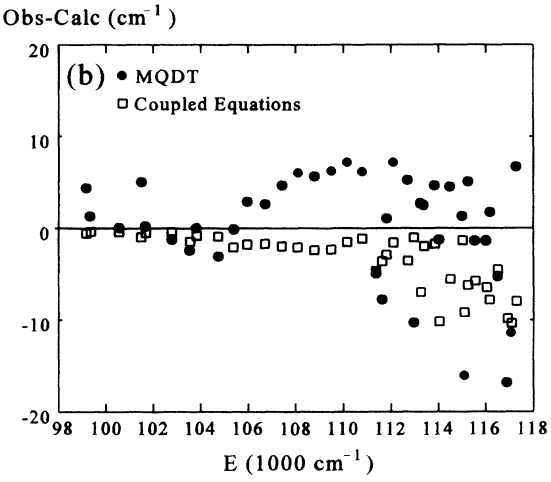

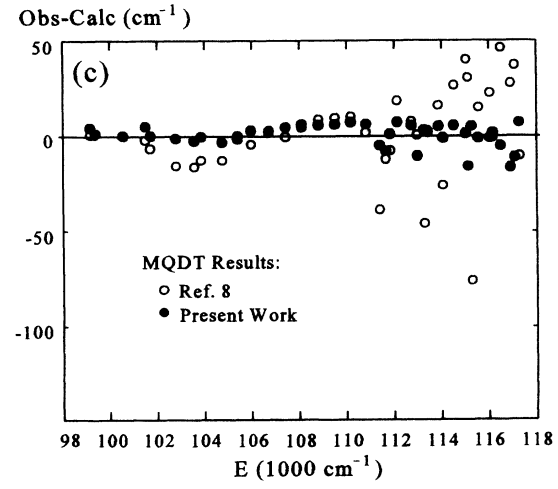

FIG. 1. Comparison of observed minus calculated vibronic energies as a function of the total vibronic energy relative to the $J=0$, $v=0$ level of the $\tilde{X}\,^1\Sigma_g^+$ ground state. (a) Comparison of the Born-Oppenheimer ("B"), Adiabatic ("A"), and MQDT (●) results. (b) Comparison of the coupled equations (Ref. [3]) (□) and MQDT (●) results. (c) Comparison of our "proof of principle" results (Ref. [8]) (○) and the present results (●).

wave functions and energies are obtained by numerical integration of the vibrational Schrödinger equation. The size of the non-Born-Oppenheimer effects in these states of H_2 is readily apparent in this figure. The root-mean-square error of the Born-Oppenheimer calculated energies for these states is about 110 cm^{-1}, compared to 6.0 cm^{-1} for the MQDT calculations. Indeed, one of the Born-Oppenheimer levels is wrong by over 500 cm^{-1}. Quadrelli, Dressler, and Wolniewicz [3,4] calculated adiabatic corrections to the potential-energy curves for these states. These corrections were as large as 800 cm^{-1} and result in a significant improvement in the calculated vibronic energies as is also seen in Fig. 1(a). However, even taking these adiabatic corrections into account resulted in an rms error of 58 cm^{-1}, with the energies of some levels calculated more than 180 cm^{-1} away from the experimental values. It is clear from this figure that the MQDT results are very much superior to those obtained in either the simple Born-Oppenheimer approximation, or in an adiabatic approximation.

Figure 1(b) compares results of nonadiabatic coupled-equations calculations performed by Yu, Dressler, and Wolniewicz [3,6] with the current MQDT results. Note the twentyfold increase in scale in Fig. 1(b) compared to 1(a). The coupled-equations results are in better agreement with experiment than are the MQDT results, however not overwhelmingly so. The rms errors are 6.0 cm^{-1} for the MQDT results *versus* 3.0 cm^{-1} for the coupled-equations results. The ranges of observed minus calculated values are $-16.8-+7.3$ cm^{-1} for the MQDT results and $-10.4--0.4$ cm^{-1} for the coupled-equations results. In comparing these calculations, it must be remembered that the MQDT results are based on the quantum-defect matrix obtained in RJ-I, which reproduces the Born-Oppenheimer potential-energy curves to within several wave-number units. We do not expect our vibronic results to be any better than this.

Figure 1(b) also shows that the MQDT results scatter more or less uniformly above and below the observed energies. This is not true of the coupled-equations results which *must* lie to higher energy than the observed levels [and so below the axis in Fig. 1(b)]. Indeed the average of the observed minus calculated energies is only $+0.3$ cm^{-1} for the MQDT results, as opposed to -3.5 cm^{-1} for the coupled-equations calculations. Examination of the figure shows that the quality of the coupled-equations results degrades more dramatically at higher energy than do the MQDT results. Dividing the results into two regions at 111 000 cm^{-1} the rms error of the MQDT degrades by a factor of only 2.2 in the higher-energy range, whereas the coupled-equations results degrade by a factor of 4.3. Indeed based on the same division of the energy range the average error improves from $2.6--1.6$ cm^{-1} for the MQDT results, but for the coupled-equations approach degrades by a factor of 4, from -1.3 to -5.4 cm^{-1}. This is possibly due to the fact that the MQDT results take into account the effect of the entire Rydberg series lying to higher energy, whereas the coupled-equations results only take into account the first five excited $^1\Sigma_g^+$ electronic states.

Figure 1(b) and Table I further show that the levels between 106 000 and 111 000 cm^{-1}, which sample large R values corresponding to the outer limb of the F state are systematically calculated about 7 cm^{-1} too low. This clearly reflects the missing correction $\frac{1}{4}(\mathcal{R}_\infty - \mathcal{R}_{H_2})$ discussed in Sec. III C 4.

In the preceding paper, we discussed how our η matrix results in a good prediction for the $4s$ diabatic state, but a much poorer one for the $4d$ state. This is also reflected in our vibronic calculations for the $v=0$ levels of the O ($\approx 4s$) and P ($\approx 4d$) $^1\Sigma_g^+(J=0)$ states wherein our prediction for the O state is in much better agreement with the recent unpublished assignments of Dressler [3] than is that for the P state. As described in RJ-I this is attributable to our present neglect of the energy dependence of η_{dd}.

V. CONCLUSION

The results displayed in the three parts of Fig. 1 demonstrate how two entirely different methods of treating strong vibronic coupling, both starting out from the same Born-Oppenheimer clamped-nuclei potential-energy curves, reproduce an extended set of experimental level energies with near-spectroscopic accuracy. The recent coupled-equations calculations by Yu, Dressler, and Wolniewicz [6] represent a significant improvement over those performed by Quadrelli, Dressler, and Wolniewicz [4]. The improvement in the Born-Oppenheimer potential curves is responsible for some of the improvement in both methods. However, for the coupled-equations method the improvement is most striking for the higher lying vibronic levels and is due to the fact that the $5\,^1\Sigma_g^+$ and $6\,^1\Sigma_g^+$ electronic states are now included, which was not possible in the earlier work. The previous MQDT calculations of Ross and Jungen [8] already implicitly contained *all* of the $^1\Sigma_g^+$ levels, including the electronic continuum lying above. The improvement obtained in the MQDT calculations, evident in Fig. 1(c), is due instead to the more careful treatment of the energy dependence of the η_{ss} defect, and possibly also due to the inclusion of the η_{sd} defect. The possibility for further improvement of the current MQDT results lies in using the new *ab initio* calculations of Wolniewicz and Dressler [5] to determine the energy dependence of the η_{dd} defect and possibly also that of the η_{pp} defect, as discussed in RJ-I.

For a more fundamental point of view, the present MQDT calculations are a striking demonstration of the power of the frame-transformation method, which has allowed us to produce the tens of thousands of elements of the rovibrational reaction matrix from the clamped-nuclei electronic quantum-defect matrix which is composed of only six smooth functions $\eta_{ij}(R)$. This success indicates that the physical picture underlying our treatment is basically correct:

(i) The doubly excited repulsive state which is usually considered as arising from the $(1\sigma_u)^2$ electronic configuration can be viewed realistically as the lowest member of the $(1\sigma_u)(np\sigma_u)$ series.

(ii) The collision between the Rydberg electron and the core is *fast*, that is, there is no trapping of the electron in-

side the core region. This behavior contrasts with that found in electron-molecule collisions, such as in $e^- + N_2$, which are often dominated by shape resonances whereby the incident electron is temporarily trapped within a potential barrier.

Our immediate goal is to use the quantum-defect matrix of RJ-I in calculations for states having J other than 0, and to continue our calculations to higher energy where the coupled-equations approach becomes more difficult to implement. The calculations for $J \neq 0$ will form the subject of the next paper in this series.

ACKNOWLEDGMENTS

S.C.R. thanks the Natural Sciences and Engineering Research Council of Canada for its support of this work. He also thanks both the ETH, Zürich, Switzerland and the late Professor Fraser Birss for support during the crucial early stages of this work. In addition, he thanks the Laboratoire Aimé Cotton du CNRS, Orsay, France, for its hospitality and assistance during many working visits. Professor Kurt Dressler is again thanked for his helpful comments and continuing provision of useful data in advance of publication, Dr. Annick Suzor-Weiner is thanked for her critical examination of this manuscript, and the assistance of the late Professor Fraser Birss with regard to the numerical evaluation of the determinants is gratefully remembered.

APPENDIX A

In this appendix we derive the three-step technique of Sec. III B for the calculation of the full rovibronic K matrix. This technique is based on the standard spectral representation of the function of an operator A, with eigenvalues a and eigenfunctions $|a\rangle$,

$$f(A) = \sum_a f(a)|a\rangle\langle a| \ . \tag{A1}$$

From the spectral representation it is straightforward to show that

$$P = \sum_i |i\rangle\langle i|, \quad f(0)=0 \ , \tag{A2}$$

P and A operate in different spaces

$$\Longrightarrow f(PA) = Pf(A) \ ,$$

where the $|i\rangle$ are orthonormal. For particular application to electronic channel mixing the following result, also based on the spectral representation, is used to handle the summation over Λ in Eq. (4)

$$f(0)=0, \quad P_\Lambda P_{\Lambda'} = 0 \ \text{ for } \Lambda \neq \Lambda' \tag{A3}$$
$$\Longrightarrow f\left(\sum_\Lambda P_\Lambda\right) = \sum_\Lambda f(P_\Lambda) \ .$$

Letting $[\![M]\!]$ denote the matrix representation of the operator M then the matrix representation $[\![f(M)]\!]$, of a function of M can be expressed by

$$U \text{ unitary} \Longrightarrow [\![f(M)]\!] = U f(U^\dagger [\![M]\!] U) U^\dagger \ . \tag{A4}$$

Equation (A4) gives rise to the technique of Sec. III B, allowing the evaluation of the full rovibronic K matrix, while bypassing the problematic integrals involving the tangent function in Eq. (15). Thus, instead of evaluating the matrix elements of $f(M)$ on the left-hand side of the equality in Eq. (A4), the matrix elements of the "bare" operator M appearing on the right-hand side of the equality are evaluated. The resulting matrix $[\![M]\!]$ is then diagonalized by the unitary matrix U and the function f is applied to the diagonal matrix $U^\dagger [\![M]\!] U$ (achieved by simply evaluating the function of the diagonal elements). The final step is to use U to transform back.

In situations involving molecular vibration the MQDT reaction matrix is nothing other than the matrix representation in the appropriate basis of the function, $f(M)=\tan\pi M$, of an operator of the form $M = \sum_\Lambda P_\Lambda A_\Lambda$. That is $K = [\![f(M)]\!]$, where the operator M depends on the particular problem. Once M has been identified application of Eq. (A4) allows the evaluation of the matrix elements of $f(M)$ and thus of K. In the remainder of this section we consider three particular cases, in order of increasing complexity, so as to more clearly illustrate the technique. We give M for each case, and verify that it satisfies $K = [\![f(M)]\!]$.

Case (a). Pure vibronic interaction (no rotation, no electronic interaction). In this case $M = \eta^\Lambda(R)$, so that $P_\Lambda = \mathbb{I}$ and $A_\Lambda = \eta^\Lambda(R)$, where Λ only takes on one value. The basis set here consists of the vibrational wave functions $|v_i^+\rangle$ of the ion core, so that the matrix representation of tangent πM is

$$[\![f(M)]\!] = [\![f(\eta^\Lambda(R))]\!] = [\![\tan\pi\eta^\Lambda(R)]\!] \ ,$$

which has elements

$$\langle v_i^+ | \tan\pi\eta^\Lambda(R) | v_j^+ \rangle = K_{v_i^+ v_j^+} \ . \tag{A5}$$

These are indeed the elements of the pure vibronic K matrix, verifying that M has been correctly chosen.

Case (b). Rovibronic interaction (no electronic interaction). This is the case for which Du and Greene [18] introduced this technique. Here $M = \sum_\Lambda |\Lambda\rangle\eta^\Lambda(R)\langle\Lambda|$, and thus $P_\Lambda = |\Lambda\rangle\langle\Lambda|$ and $A_\Lambda = \eta^\Lambda(R)$. The basis functions now include a rotational part and are $|v_i^+ N_i^+\rangle$. Because $P_\Lambda P_{\Lambda'} = 0$ if $\Lambda \neq \Lambda'$, Eq. (A3) may be applied to M. Then, using Eq. (A2), the matrix representation of tangent πM is

$$[\![f(M)]\!] = \left[\!\!\left[f\left(\sum_\Lambda P_\Lambda A_\Lambda\right)\right]\!\!\right]$$
$$= \left[\!\!\left[\sum_\Lambda f(P_\Lambda A_\Lambda)\right]\!\!\right] = \left[\!\!\left[\sum_\Lambda P_\Lambda f(A_\Lambda)\right]\!\!\right] , \tag{A6}$$

which has elements

$$\langle v_i^+ N_i^+ | \left\{ \sum_\Lambda |\Lambda\rangle \tan\pi\eta^\Lambda(R) \langle\Lambda| \right\} |v_j^+ N_j^+\rangle$$

$$= \sum_\Lambda \langle N_i^+|\Lambda\rangle \langle v_i^+; N_i^+ | \tan\pi\eta^\Lambda(R) | v_j^+; N_j^+\rangle \langle\Lambda|N_j^+\rangle$$

$$= K_{v_i^+ N_i^+, v_j^+ N_j^+} ,$$

which are indeed those of the rovibronic K matrix of Eq. (5) of Du and Greene [18] [equivalent to Eq. (29) of JA], verifying the choice of M.

Case (c). Rovibronic interaction with electronic interaction (present work). In this case $M = \sum_\Lambda |\Lambda\rangle \{ \sum_\alpha |\alpha\rangle^\Lambda \eta_\alpha^\Lambda(R)^\Lambda \langle\alpha|\} \langle\Lambda|$, so that $P_\Lambda = |\Lambda\rangle\langle\Lambda|$ and $A_\Lambda = \sum_\alpha |\alpha\rangle^\Lambda \eta_\alpha^\Lambda(R)^\Lambda\langle\alpha|$, where $|\alpha\rangle^\Lambda$ are the eigenfunctions and η_α^Λ the related eigenquantum defects of the electronic K^Λ matrix obtained in Eq. (16). The basis functions now additionally include an electronic part and are $|iv_i^+ N_i^+\rangle$. Again, because $P_\Lambda P_{\Lambda'} = 0$ when $\Lambda \neq \Lambda'$, Eqs. (A3) and (A2) may be applied to M, resulting in an expression containing $f(A_\Lambda)$. The special feature here is that A_Λ itself has the form $A_\Lambda = \sum_\alpha P_\alpha^\Lambda \eta_\alpha^\Lambda(R)$, where $P_\alpha^\Lambda = |\alpha\rangle^\Lambda{}^\Lambda\langle\alpha|$, and thus Eqs. (A3) and (A2) can be applied once more, this time to $f(A_\Lambda)$. Doing this the matrix representation of tangent πM is

$$[\![f(M)]\!] = \left[\!\!\left[f\left(\sum_\Lambda P_\Lambda A_\Lambda \right) \right]\!\!\right] = \left[\!\!\left[\sum_\Lambda f(P_\Lambda A_\Lambda) \right]\!\!\right] = \left[\!\!\left[\sum_\Lambda P_\Lambda f(A_\Lambda) \right]\!\!\right]$$

$$= \left[\!\!\left[\sum_\Lambda P_\Lambda f\left(\sum_\alpha P_\alpha^\Lambda \eta_\alpha^\Lambda \right) \right]\!\!\right] = \left[\!\!\left[\sum_\Lambda P_\Lambda \sum_\alpha P_\alpha^\Lambda f(\eta_\alpha^\Lambda) \right]\!\!\right] ,$$

which has elements

$$\langle iv_i^+ N_i^+ | \sum_\Lambda |\Lambda\rangle \left\{ \sum_\alpha |\alpha\rangle^\Lambda \tan\pi\eta^\Lambda(R)\, {}^\Lambda\langle\alpha| \right\} \langle\Lambda||jv_j^+ N_j^+\rangle$$

$$= \sum_\Lambda \langle iv_i^+ N_i^+ || \Lambda\rangle |i\rangle \left\{ \sum_\alpha \langle i|\alpha\rangle^\Lambda \tan\pi\eta^\Lambda(R)\, {}^\Lambda\langle\alpha|j\rangle \right\} \langle j|\langle\Lambda||jv_j^+ N_j^+\rangle$$

$$= \sum_\Lambda \langle iv_i^+ N_i^+ || \Lambda\rangle |i\rangle K_{ij}^\Lambda(R) \langle j|\langle\Lambda||jv_j^+ N_j^+\rangle$$

$$= \int dR \langle iv_i^+ N_i^+ | \left\{ \sum_\Lambda |iR\Lambda\rangle K_{ij}^\Lambda(R) \langle jR\Lambda| \right\} |jv_j^+ N_j^+\rangle$$

$$= K_{iv_i^+ N_i^+, jv_j^+ N_j^+} , \tag{A7}$$

which are indeed those of the full rovibronic K matrix of Eq. (4) for arbitrary JM values, thereby verifying that M has been correctly chosen. (The introduction of $|i\rangle\langle i|$ and $|j\rangle\langle j|$ in the second step is valid due to the presence of $\langle i|$ and $|j\rangle$ in $\langle iv_i^+ N_i^+|$ and $|jv_j^+ N_j^+\rangle$.) $\langle i|\alpha\rangle^\Lambda$ is the $i\alpha$ element of the diagonalizing transformation V^Λ of Eq. (16).

Having determined M for each of these cases the evaluation of the rovibronic K matrix proceeds using Eq. (A4),

$$K = [\![f(M)]\!] = U f(U^\dagger [\![M]\!] U) U^\dagger ,$$

where $[\![M]\!]$ has elements

$$\begin{aligned}
&\text{case (a)} \quad \langle v_i^+ | \eta^\Lambda(R) | v_j^+ \rangle , \\
&\text{case (b)} \quad \sum_\Lambda \langle N_i^+|\Lambda\rangle \langle v_i^+; N_i^+ | \eta^\Lambda(R) | v_j^+; N_j^+\rangle \langle\Lambda|N_j^+\rangle , \\
&\text{case (c)} \quad \sum_\Lambda \langle N_i^+|\Lambda\rangle \langle v_i^+; iN_i^+ | \left\{ \sum_\alpha \langle i|\alpha\rangle^\Lambda \eta_\alpha^\Lambda(R)\, {}^\Lambda\langle\alpha|j\rangle \right\} |v_j^+; jN_j^+\rangle \langle\Lambda|N_j^+\rangle ,
\end{aligned} \tag{A8}$$

and U is chosen in each case so that $U^\dagger [\![M]\!] U$ is diagonal. The right-hand side of the equality in Eq. (A8) is used to evaluate the vibronic K matrix. This is done by first evaluating the elements of the matrix representation of M. The result is the matrix $[\![M]\!]$ in Eq. (A8), which, for case (c) is also given by Eq. (17). This is step 2 of the three-step process of Sec. III B. Step 3 is then to diagonalize $[\![M]\!]$ by the unitary matrix U, take tangentπ of each element of the resulting diagonal matrix $U^\dagger [\![M]\!] U$, and finally to transform back with the U matrix again, as shown at the top of Eq. (A8) and in Eq. (18). In this way the K matrix may be evaluated without having to integrate over the tangent function.

APPENDIX B

In this appendix we briefly describe our *ab initio* calculation of the adiabatic corrections for the $1\sigma_u$ state of H_2^+. Because of the modest nature of our requirements *vis a vis* precision (the order of a wave-number unit is satisfactory) we did not implement the procedure of Ponomarev, Puzynina, and Truskova [29], and instead proceeded by Simpson's rule integration, using the H_2^+ electronic wave functions of Bates, Ledsham, and Stewart [28] in Eqs. (4) and (6) of Bishop *et al.* [30] [with the correction that the sum on j in their expression for $M(\mu)$ should be from $\Lambda+l$ and not from Λ. This correction is needed in order to obtain equal adiabatic corrections for the $1\sigma_g$ and $1\sigma_u$ states at $R=\infty$, expected as these two steps converge to the same H($1s$)+H($2s$) limit]. In this integration the $\partial/\partial\mu$ derivatives were evaluated numerically and the $\partial/\partial\lambda$ derivatives analytically. The calculation was done on a coarse grid of R values from 0.8–8.0 a.u., with other values obtained by splining, as was done for the $1\sigma_g$ state. The number of points and the range of integration over λ were adjusted to achieve reasonable numerical convergence. As a check we used the same program to calculate the adiabatic corrections for the $1\sigma_g$ state to compare with the values obtained by Bishop and Wetmore [20]. In the range $R=0.6$–6.0 a.u. our calculations agree with theirs to within better than 1 μa.u. (0.2 cm^{-1}), thus providing some confidence in our calculations for the $1\sigma_u$ state. The $R\to\infty$ value of the adiabatic correction for both states, $-m_e E(\infty)/M_p$ (M_P denotes mass of proton), was used to fix the adiabatic corrections at large R. For the purposes of splining the asymptotic value was used to fix the corrections at $R=100$ a.u.

The expectation values of the two terms of $H^{\rm Ion}_{\rm missing}$ in the limit $R\to\infty$ provides another check on the precision of our adiabatic corrections. JA point out that since the work of Van Vleck [21] it is known that in this limit the expectation values of these two terms become equal, and thus each becomes equal to half of the total asymptotic value. For the $1\sigma_g$ and $1\sigma_u$ states, the asymptotic limit for each of these terms is thus 136 μa.u. At $R=8$ a.u. Bishop *et al.* [30] obtain 135 and 133 μa.u., whereas our more approximate calculations give 137 and 134 μa.u. This comparison serves to indicate both the precision of our calculations at large R and also roughly how close to equality the two terms should be. Thus, our results of 131 and 136 μa.u. for these two terms for the $1\sigma_u$ state at $R=8$ a.u. are seen to be quite reasonable.

APPENDIX C

The derivative correction to the quantum defect, forming part of $\langle H^{\rm Rydberg}_{\rm missing}\rangle$, is obtained in an electronically diagonal approximation. Additionally putting aside any energy dependence of the quantum defects, the single electronic channel Eq. (4) of RJ-I

$$0=\tan\pi\nu+A(\nu)\tan\pi\eta\ , \tag{C1}$$

establishes the relationship between the energies ϵ [through ν in Eq. (3) of RJ-I] and the quantum defects η. To effect a change of $\Delta\epsilon$ on an energy satisfying Eq. (C1) would require a change of η of approximately

$$\Delta\eta\approx\frac{\partial\eta}{\partial\epsilon}\Delta\epsilon\ , \tag{C2}$$

where $\partial\eta/\partial\epsilon$ does not refer to any energy dependence of the quantum defects (which we neglect here), but instead to the relation between η and ϵ implicit in Eq. (C1). The change desired in ϵ is that given by the second term of Eq. (24),

$$\Delta\epsilon=-\frac{1}{4\mu}R\frac{\partial\epsilon}{\partial R}\ , \tag{C3}$$

and, thus, the correction to the diagonal quantum defects is given by

$$\Delta\eta=-\frac{1}{4\mu}R\frac{\partial\eta}{\partial\epsilon}\frac{\partial\epsilon}{\partial R}=-\frac{1}{4\mu}R\frac{\partial\eta}{\partial R}\ . \tag{C4}$$

[1] S. C. Ross and Ch. Jungen, preceding paper, Phys. Rev. A **49**, 4353 (1994).
[2] L. Wolniewicz and K. Dressler, J. Chem. Phys. **82**, 3292 (1985).
[3] K. Dressler (private communication).
[4] P. Quadrelli, K. Dressler, and L. Wolniewicz, J. Chem. Phys. **92**, 7461 (1990).
[5] L. Wolniewicz and K. Dressler, J. Chem. Phys. **100**, 444 (1994).
[6] S. Yu, K. Dressler, and L. Wolniewicz (unpublished).
[7] Ch. Jungen and O. Atabek, J. Chem. Phys. **66**, 5584 (1977).
[8] S. Ross and Ch. Jungen, Phys. Rev. Lett. **59**, 1297 (1987).
[9] M. J. Seaton, Rep. Prog. Phys. **46**, 167 (1983).
[10] U. Fano, Phys. Rev. A **2**, 353 (1970).
[11] G. Herzberg and Ch. Jungen, J. Mol. Spectrosc. **41**, 425 (1972).
[12] E. S. Chang, D. Dill, and U. Fano, in *Abstracts of Papers, Proceedings of the Eighth International Conference on the Physics of Electronic and Atomic Collisions,* edited by B. C. Cobic and M. V. Kurepa (Institute of Physics, Belgrade, 1973), p. 536.
[13] C. H. Greene, Comments At. Mol. Phys. **23**, 209 (1989).
[14] C. H. Greene and Ch. Jungen, Adv. At. Mol. Phys. **21**, 51 (1985).
[15] P. R. Bunker, *Molecular Symmetry and Spectroscopy* (Academic, New York, 1979).
[16] E. S. Chang and U. Fano, Phys. Rev. A **6**, 173 (1972).
[17] M. S. Child and Ch. Jungen, J. Chem. Phys. **93**, 7756 (1990).
[18] N. Y. Du and C. H. Greene, J. Chem. Phys. **85**, 5430 (1986).

[19] H. Gao and C. H. Greene, J. Chem. Phys. **91**, 3988 (1989).
[20] D. M. Bishop and R. W. Wetmore, Mol. Phys. **26**, 145 (1973).
[21] J. H. Van Vleck, J. Chem. Phys. **4**, 327 (1936).
[22] John C. Slater, *Quantum Theory of Molecules and Solids,* Electronic Structure of Molecules Vol. I (McGraw-Hill, New York, 1963).
[23] L. Wolniewicz and T. Orlikowski, Mol. Phys. **74**, 104 (1991).
[24] J. W. Cooley, Math. Comp. **15**, 363 (1961).
[25] E. R. Cohen and B. N. Taylor, *The 1986 Adjustment of the Fundamental Physical Constants,* report of CODATA Task Group on Fundamental Constants, CODATA Bulletin 63 (Pergamon, Elmsford, New York, 1986).
[26] W. Kołos, K. Szalewicz, and H. J. Monkhorst, J. Chem. Phys. **84**, 3278 (1986).
[27] H. Wind, J. Chem. Phys. **42**, 2371 (1965).
[28] D. R. Bates, K. Ledsham, and A. L. Stewart, Phil. Trans. R. Soc. London, Ser. A **246**, 215 (1953).
[29] L. I. Ponomarev, T. P. Puzynina, and N. F. Truskova, J. Phys. B **22**, 3861 (1978).
[30] D. M. Bishop, Shing-Kuo Shih, C. L. Beckel, Fun-Min Wu, and J. M. Peek, J. Chem. Phys. **63**, 4836 (1975).